PNAS
www.pnas.org

Supplementary Information for

High-throughput selection of cells based on accumulated growth and division using PicoShell Particles

Mark van Zee[1], Joseph de Rutte[1], Rose Rumyan[1], Cayden Williamson[1], Trevor Burnes[2] Randor Radakovits[3], Andrew Sonico Eugenio[4], Sara Badih[1], Sohyung Lee[1], Dong-Hyun Lee[5], Maani Archang[1], Dino Di Carlo[*1, 6, 7, 8]
[1]Department of Bioengineering, University of California, Los Angeles
[2]Department of Chemical and Biomolecular Engineering, University of California, Los Angeles
[3]Synthetic Genomics Inc., San Diego, CA, USA
[4]Department of Computer Science and Engineering, University of California, Los Angeles
[5]Psycology Department, University of California, Los Angeles
[6]Deparment of Mechanical and Aerospace Engineering, University of California, Los Angeles
[7]California NanoSystems Institute, University of California, Los Angeles
[8]Jonsson Comprehensive Cancer Center, University of California, Los Angeles

*Dino Di Carlo
Email: dicarlo@ucla.edu

This PDF file includes:

Other supplementary materials for this manuscript include the following:

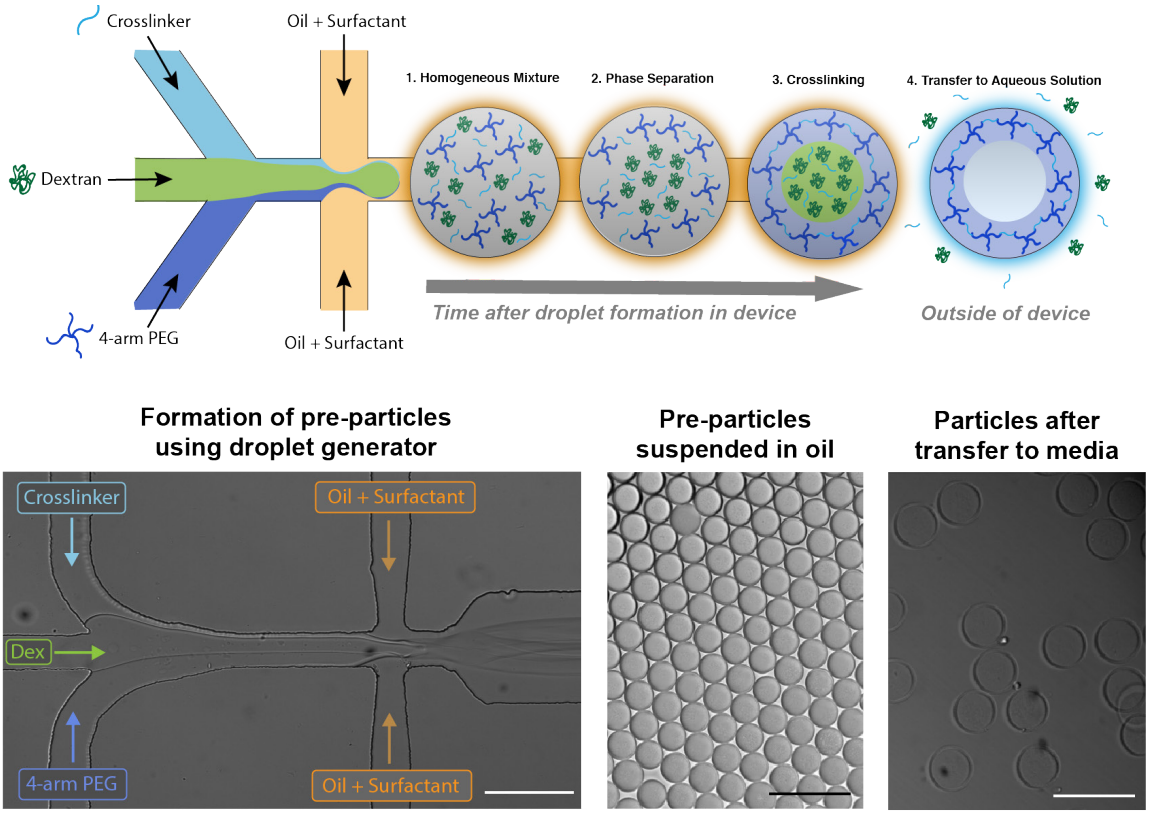

Figure S1. Microfluidic fabrication of PicoShells. PicoShells are formed by mixing together crosslinker, dextran, and 4-arm PEG to form a water-in-oil droplet emulsion. The reagents are mixed at the point of droplet formation to reduce premature gelation and phase separation. There is initially a homogeneous mixture of reagents, but the 4-arm PEG and dextran phases separate as the droplet travels down the channel. It is likely that the crosslinker remains uniformly distributed throughout the droplet. As 4-arm PEG and dextran separate, the crosslinker and 4-arm PEG react. Following gelation, the particles are phase transferred from oil to aqueous solution where dextran and un-reacted crosslinker leaks out of the particles via pores in the outer shell. The outer diameter of PicoShells is larger than that of pre-particles (~90 μm and ~70 μm respectively) due to the expected swelling of the PEG hydrogel in aqueous solutions. Scale bars = 200 μm.

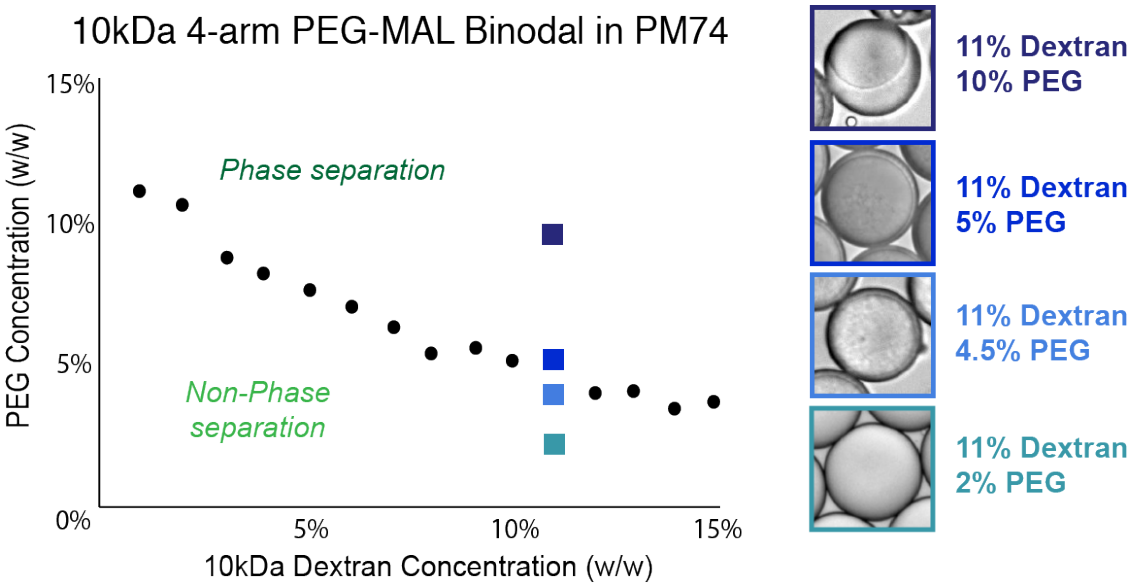

Figure. S2. Phase diagram of 10kDa 4-arm PEG-maleimide and 10 kDa dextran in PM74 seawater medium. Black dots represent concentrations we experimentally determined where the binodal is located through visual observation of droplets with varying concentrations of PEG and Dextran. PEG and dextran with concentrations below the binodal curve do not undergo phase separation, resulting in solid hydrogel particles. At PEG and dextran concentrations above the curve the droplets phase separate into PEG rich and dextran rich regions. The resulting morphology is dictated by the balance of interfacial tensions between the PEG, dextran and oil phases and the resulting particle shape is dictated by the cross-linkable PEG rich region. It was found that at higher PEG and Dextran concentrations (11% Dextran, 10% PEG) the Dextran rich region partially wets the oil interface resulting in bowl shaped particles. At lower concentrations the PEG rich region completely wets the oil interface resulting in fully enclosed Picoshells In general it was found that PEG and dextran concentrations 0.5-2% above and to the right of the points of the binodal curve result in the desired Picoshell morphology.

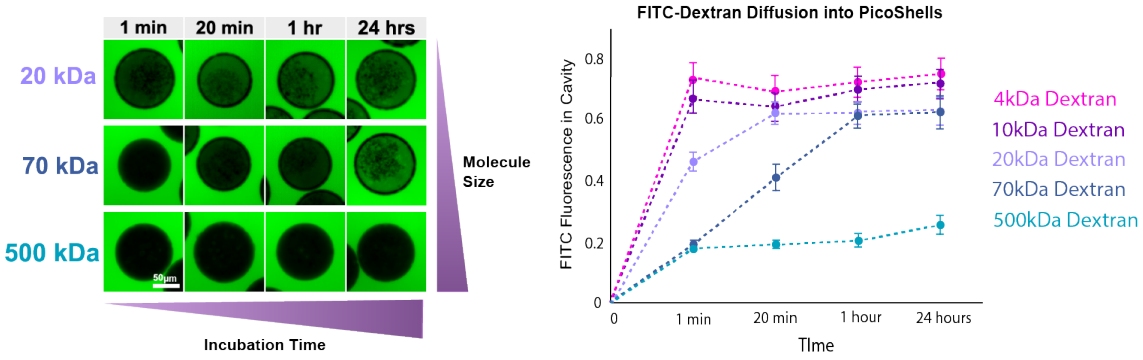

Figure S3. Characterization of diffusion through the outer hydrogel matrix of the Picoshells. The rate at which molecules diffuse through the PicoShell's outer matrix depends on the size of the molecules. PicoShells were placed into solutions containing FITC-dextran (green) of various molecular weights and the transport of those molecules into the PicoShell cavity was tracked over time. For FITC-dextran ≤ 20kDa we observe rapid entry into the cavity (i.e. equilibrium within 20min). 70kDa FITC-dextran diffuses more slowly into the cavity, reaching equilibrium at between 1 and 24h. 500kDa FITC-dextran was not seen to enter into the PicoShell cavity even after 24h. Error bars represent standard deviation in the fluorescence measurements between PicoShells in each sample. 50 particles were measured for each sample. Scale bar = 50 μm.

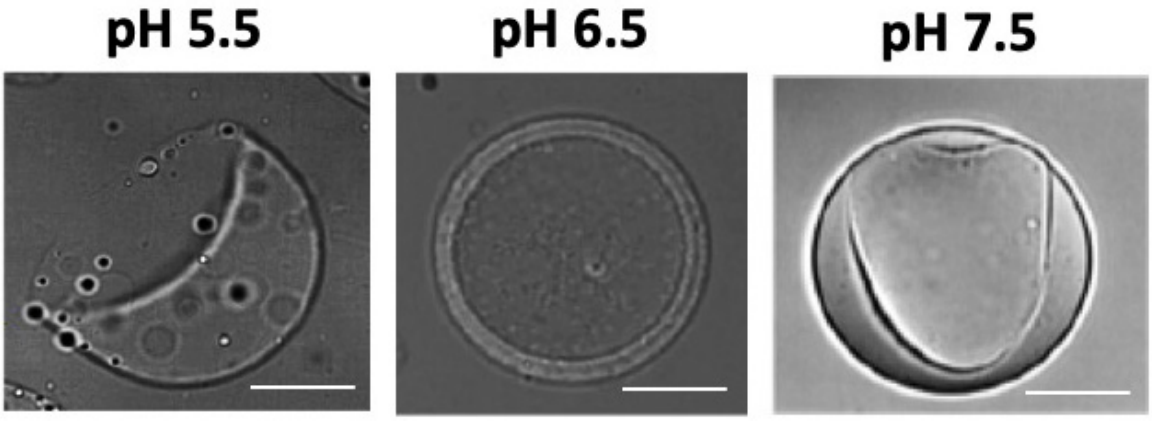

Figure S4. Sensitivity of particle shape to crosslinking rate. The rate of crosslinking was varied by adjusting the pH of the precursor solution from 5.5 – 7.5 for a fixed PEG and dextran concentration. At a pH of 7.5, the time between droplet formation and crosslinking occurs too quickly, resulting in polymerization before the PEG and dextran are able to phase separate completely and form a uniform hollow shell structure. At a pH of 5.5, crosslinking rate is reduced resulting in formation of janus particles. We theorize that in the initial phase of crosslinking the effective molecular weight of the PEG monomers increases as they link together leading to a shift in the binodal which changes the equilibrium morphology. At a pH of 6.5 we found that the crosslinking rate is slow enough to alow for complete phase separation and quick enough to preserve the ideal PicoShell morphology. Scale bar = 25μm.

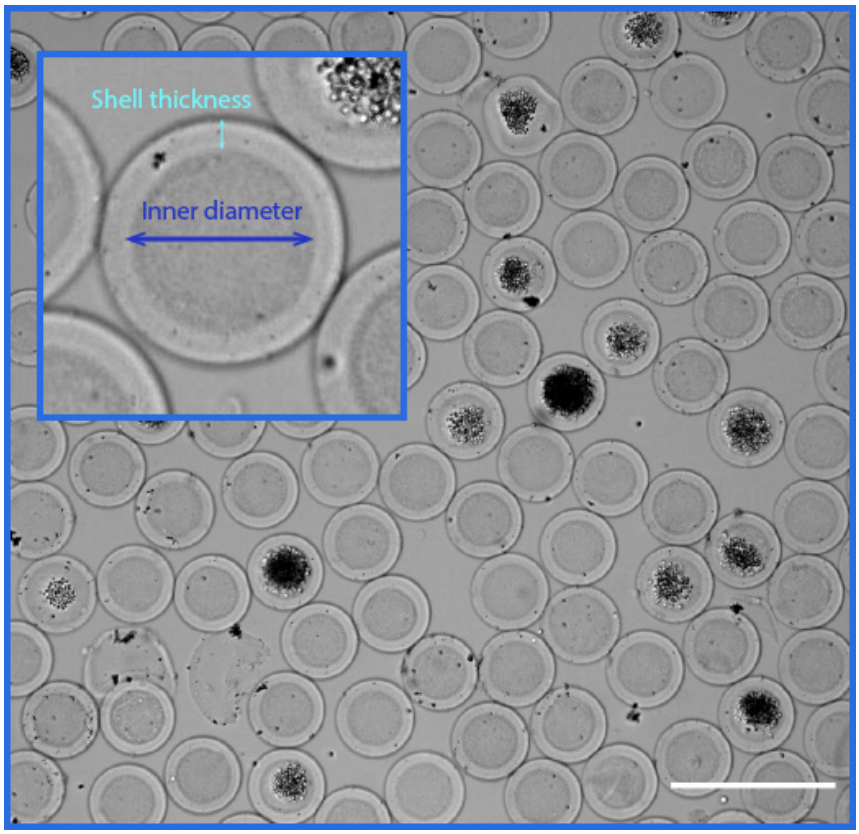

Figure S5. PicoShells fabricated with encapsulated *Chlorella* colonies are highly uniform in size and morphology. PicoShells have an average outer diameter of 90.7μm with a CV of 1.7%. The particles also have an average shell thickness of 12.7μm with a CV of 6.9%. Scale bar = 200 μm.

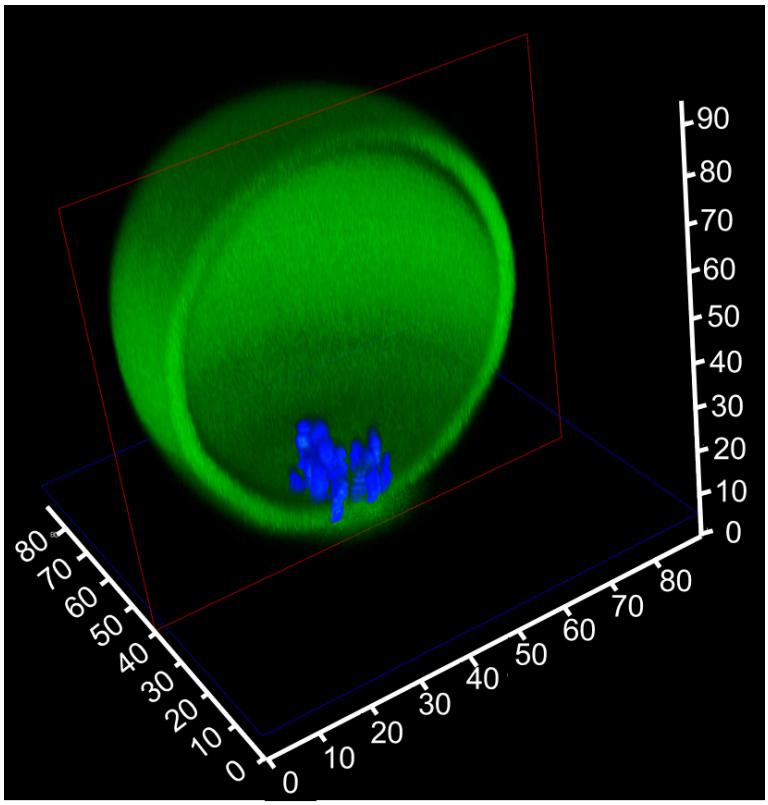

Figure S6. Confocal microscopy image of a cell-loaded PicoShell. *S. cerevisiae are* stained with CellTracker™ Deep Red Dye (blue) and encapsulated into PicoShell stained with Alexa Flour™ 488 Maleimide (green). Cells fall to the bottom of the PicoShell when at rest.

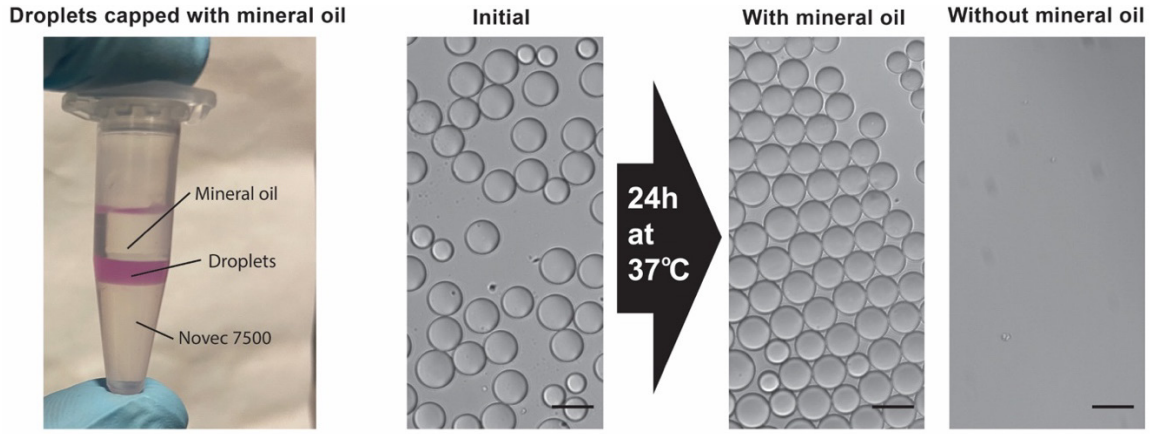

Figure S7. Effects of mineral oil cap on droplet stability. Droplets containing adherent CHODP12 media were formed using standard droplet generation techniques. One sample was capped with mineral oil the other was not capped. After 24h in the incubator at 37°C, droplets that were capped with mineral oil remained stable while droplets not capped with mineral oil de-stabilized. Scale bars = 100 µm.

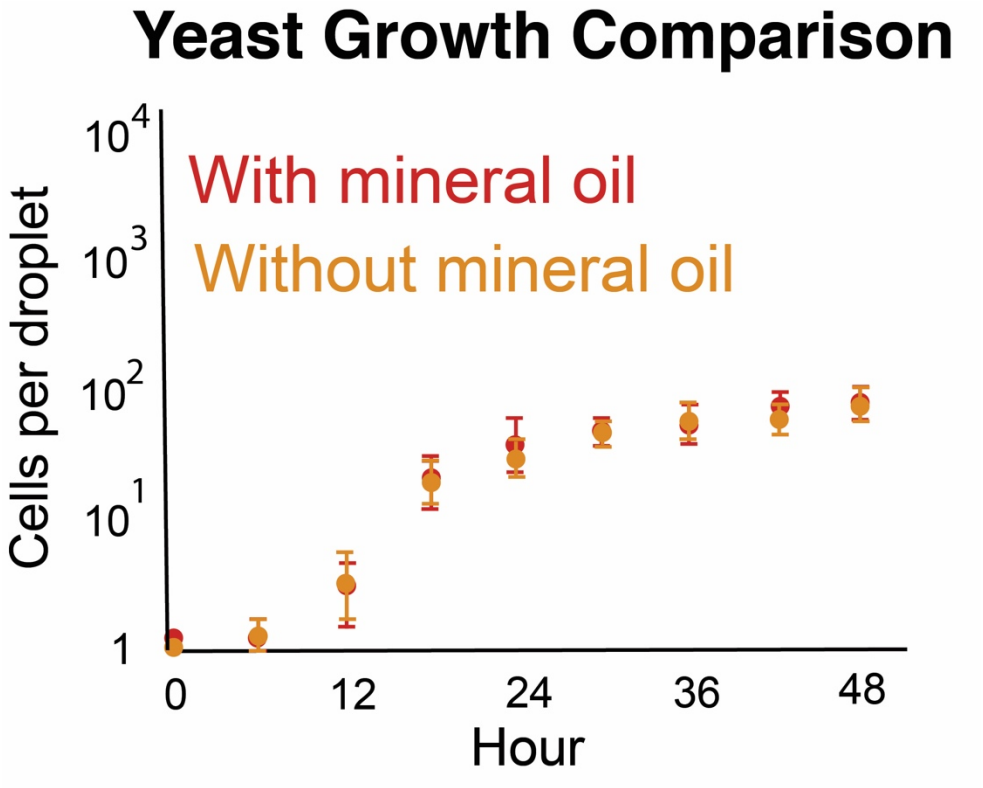

Figure S8. Mineral oil growth comparison. *S. cerevisiae* from the same culture was encapsulated into droplets. Half of the sample was placed separate from the other half and covered in mineral oil as shown in Figure S7. Growth of cells over a 48h period was tracked. We found that there is no statistically significant difference ($P > 0.05$) of the growth of *S. cerevisiae* in droplets covered with mineral oil versus without mineral oil. 5000-6000 cell-containing droplets were counted for each sample.

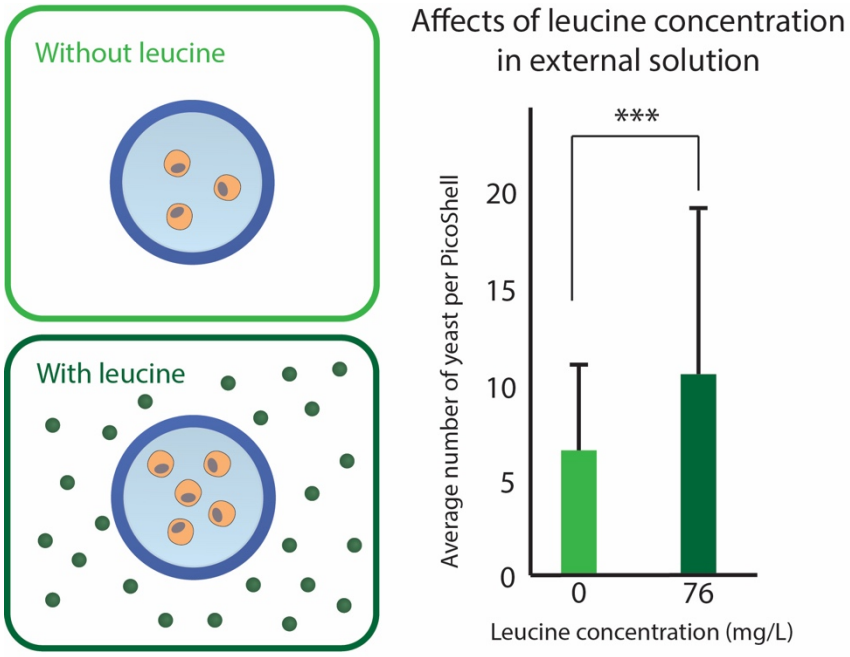

Figure S9. Leucine replenishment in PicoShells. *S. cerevisiae* shows a statistically significant growth increase ($P < 0.001$) over a 12h period when placed in a solution supplemented with 76mg/L leucine versus a solution without leucine. Error bars represent the standard deviation in the number of yeast cells per PicoShell. 300 cell-containing PicoShells were counted for each sample.

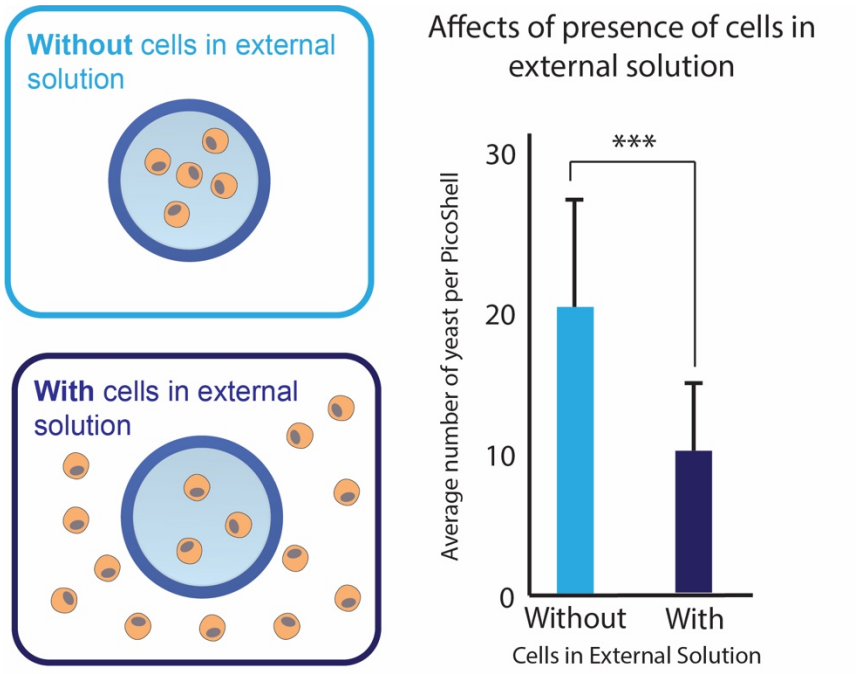

Figure S10. Effects of cells in external solution on growth in PicoShells. *S. cerevisiae* shows a statistically significant growth decrease ($P < 0.001$) over a 12h period when placed in a solution supplemented with 100 million cells/mL versus a solution without cells. Cells in external solution only grew 17% over the same period, presumably because of quruom sensing factors released due to the high desnity of cells. It is likely that these same factors diffused into the PicoShells and altered the growth and division properties of the enclosed cells. Error bars represent the standard deviation in the number of yeast cells per PicoShell. 300 cell-containing PicoShells were counted for each sample.

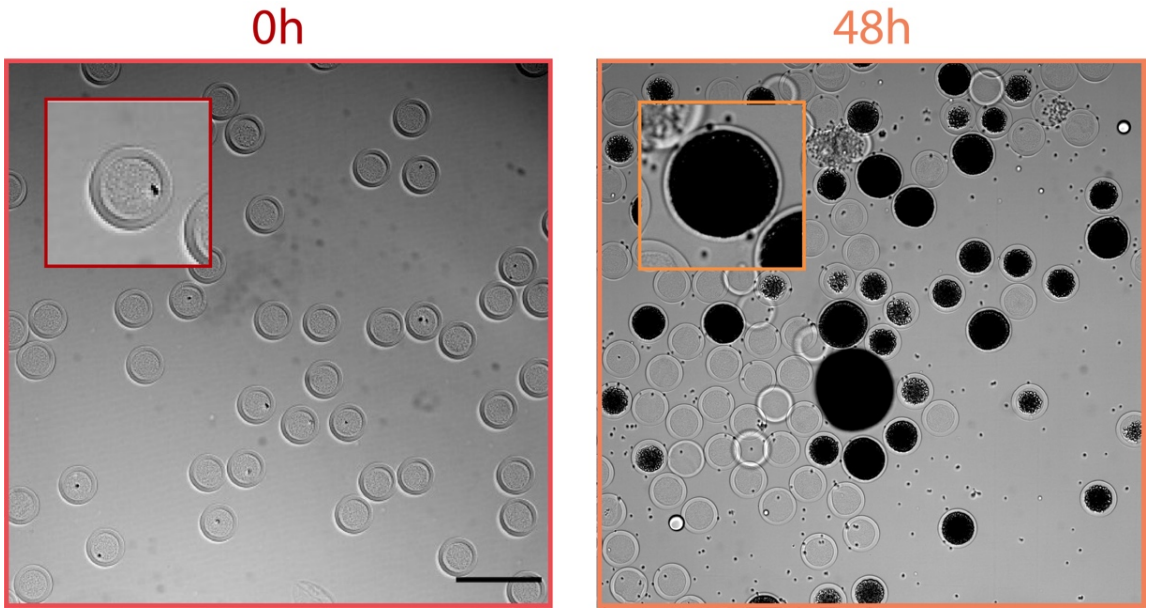

Figure S11. Expansion of PicoShells due to *S. cerevisiae* cell growth. (Left) PicoShells containing CHODP12 cells immediately after encapsulation have the same outer diameter as empty PicoShells (80μm OD, 2.1% CV). Inset shows PicoShell containing a single CHODP12 cell. (Right) As the CHODP12 cells grow the PicoShells were found to stretch and increase in diameter (122μm OD, 27.2% CV after 2 weeks). Inset shows a PicoShell containing >15000 cells that expanded from a single clone. Scale bar = 200μm.

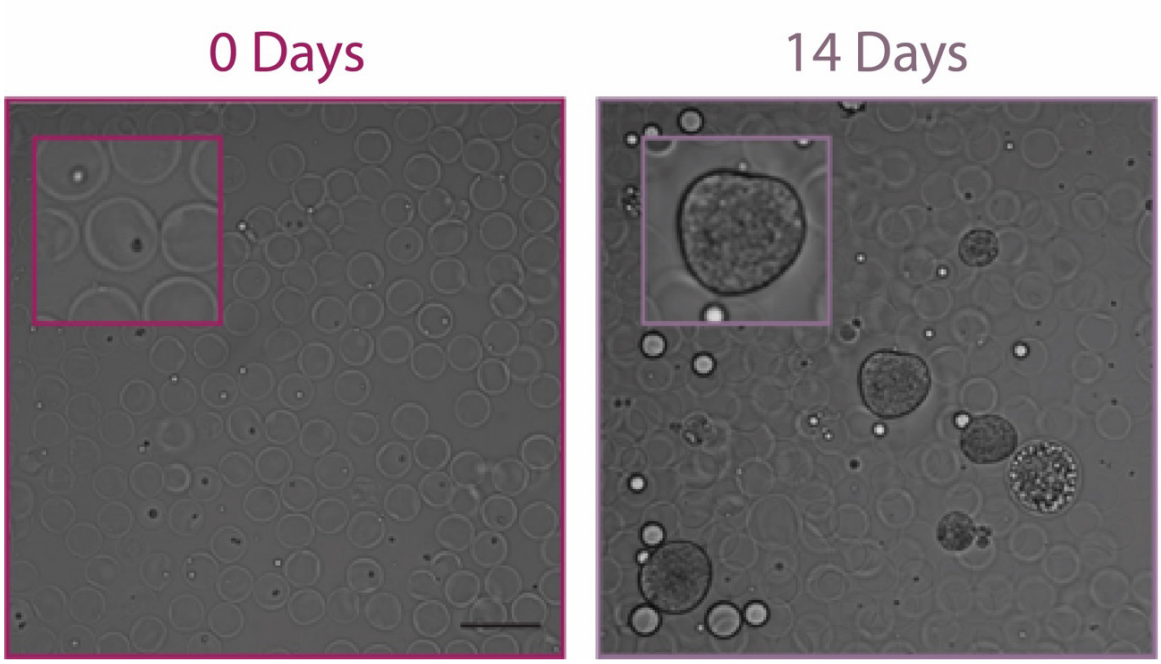

Figure S12. Expansion of PicoShells due to CHO cell growth. (Left) PicoShells containing CHODP12 cells immediately after encapsulation have the same outer diameter as empty PicoShells (80μm OD, 2.1% CV). Inset shows PicoShell containing a single CHODP12 cell. (Right) As the CHODP12 cells grow the PicoShells were found to stretch and increase in diameter (122μm OD, 27.2% CV after 2 weeks). Scale bar = 200μm.

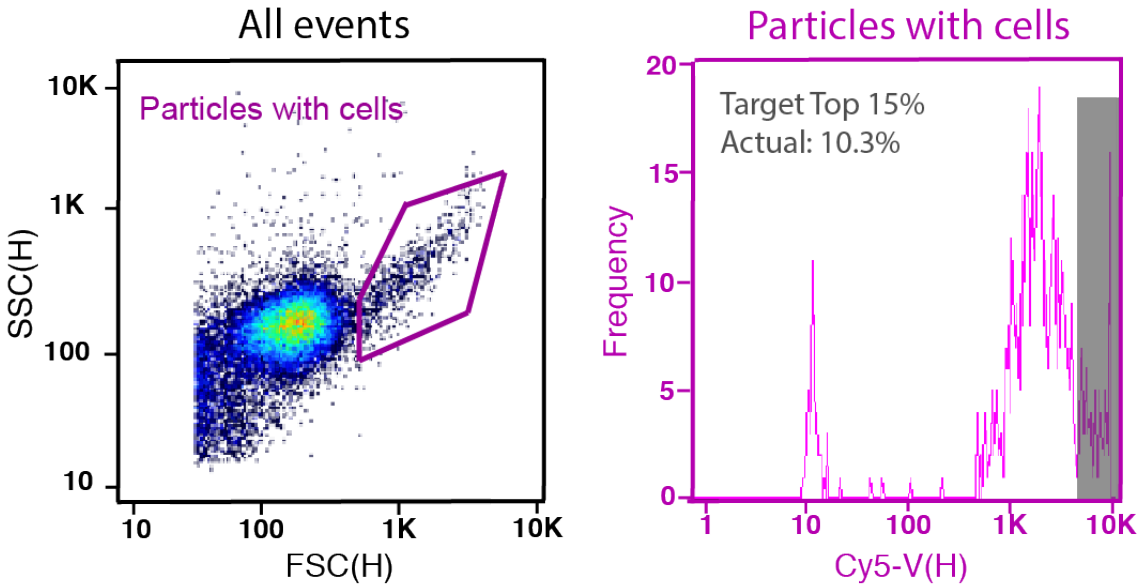

Figure S13. Full selection FACS data. For the full selection of hyperperforming *Chlorella* colonies, we first gated events that produced high scatter signal (purple gate) and sorted events that produced the highest 15% [Cy5-V(H)] signal. The data presented only shows 14,854 of the 121,213 PicoShells that were screened for the selection.

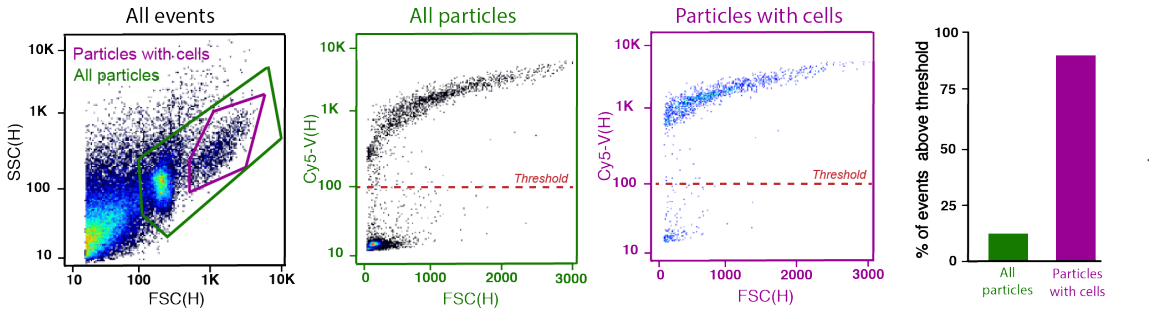

Figure S14. Additional *Chlorella*-containing PicoShell screening data. PicoShells containing *Chlorella* clonal colonies produce 3 distinct [FSC(H)] vs [SSC(H)] readout populations: one for particles containing colonies, one for empty particles, and one for debris. When all particles are gated, there are two distinct populations on a [FSC(H)] vs [Cy5-V(H)] plot, one population with a low [Cy5-V(H)] readout and another population with higher [Cy5-V(H)] readouts. When we gate the high scatter readouts from the [FSC(H)] vs [SSC(H)] plot, we find that this population corresponds to PicoShells that produce the highest [Cy5-V(H)] readouts. When all particles are gated, 14.1% of events are above a 100 [Cy5-V(H)] readout. When the high scatter population is gated, 89.9% of events are above a 100 [Cy5-V(H)] readout. Since we anticipate that colony-containing PicoShells will produce high scatter signal (as observed in an inverted microscope) and high Cy5 fluorescence signal due to a *Chlorella's* chlorophyll autofluorescence, we infer that this high scatter, high Cy5 population corresponds to colony-containing PicoShells. When we gate for 'Particles with cells' on the [FSC(H)] vs [SSC(H)] plot, we obtain a 94.0% purity and 72.7% yield of colony-containing PicoShells.

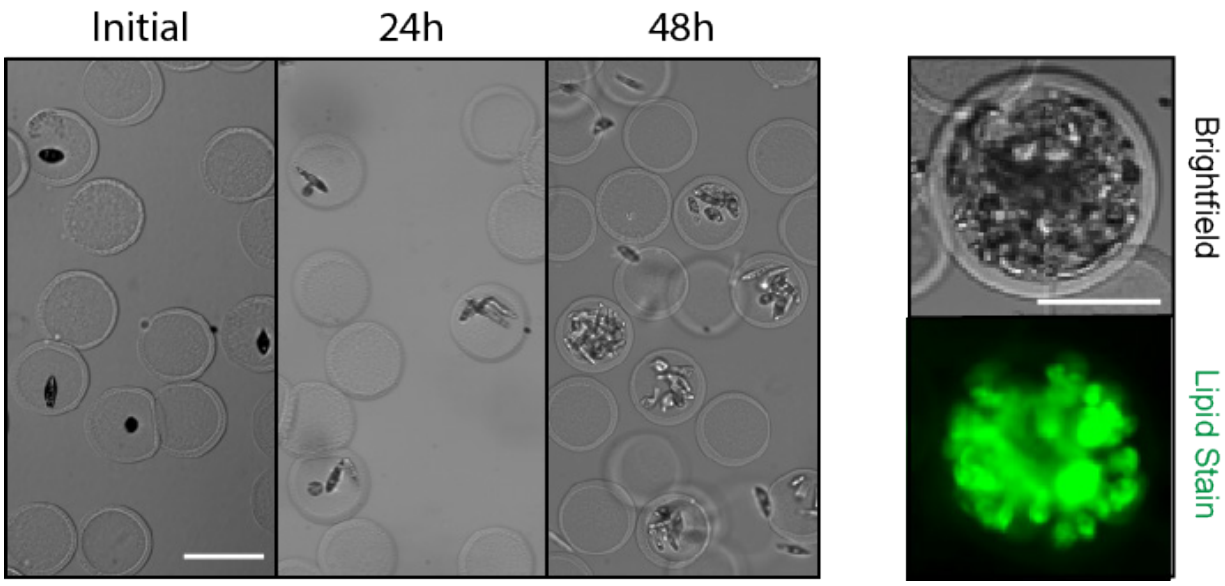

Figure S15. *Euglena gracilis* biomass and lipid accumulation within hollow shell particles. (a) Euglena cells were encapsulated into non-degradable hollow shell particles and allowed to grow over a 2-day period. We demonstrated that Euglena are viable and can accumulate biomass within hollow shell particles over this period. Particles were exchanged into a solution with BODIPY after the 2-day incubation to fluorescently label wax esters within the encapsulated microalgae. Stains were able to transport through the solid polymer matrix of the hollow particles and label cells without sticking a significant amount to the particle's PEG surface. Scale bars = 100μm.

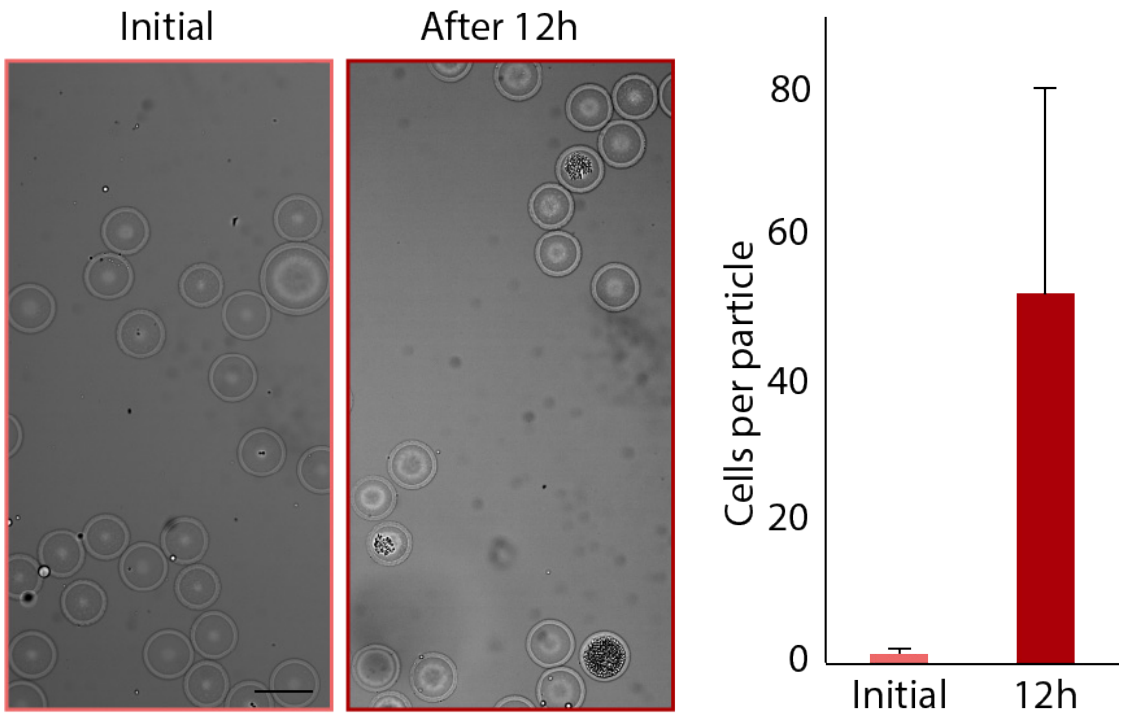

Figure S16. Growth of yeast in di-sulfide cross-linked particles. *S. cerevisiae* were encapsulated into PicoShells crosslinked with 20kDa PEG-OPSS and DTT, such that the particle's outer shell contains chemically degradable di-sulfide linkages. Yeast encapsulated into these particles were able to remain viable and multiply, increasing from an average 1.5 cells/PicoShell to 51.4 cells/PicoShell in 12h. Error bars represent the standard deviation in the number of cells between PicoShells in each sample. 150 cell-containing PicoShells were counted for each sample. Scale bar = 100μm.

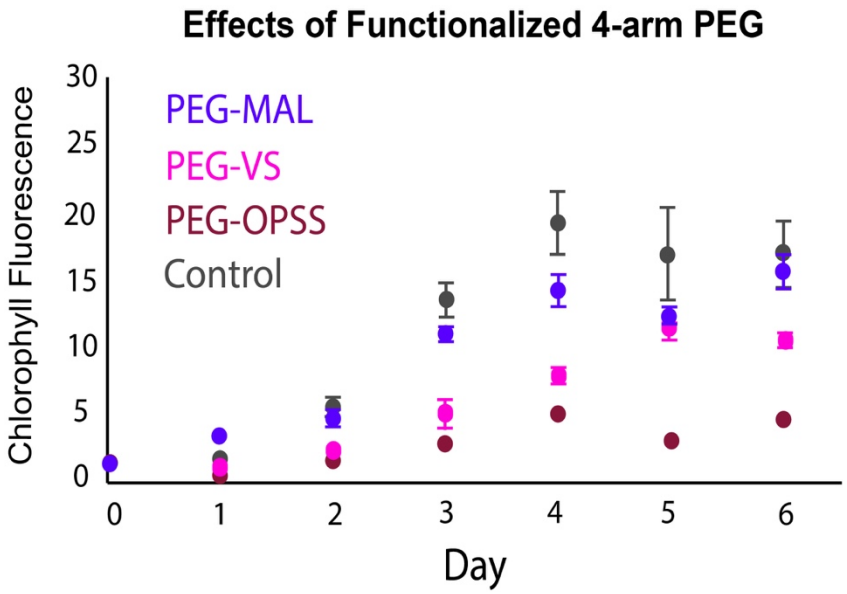

Figure S17. Effects of functionalized 4-arm PEG on *Chlorella* viability. *Chlorella* were incubated with 5% (w/w) 10kDa 4-arm PEG-malemide (MAL), 10kDa 4-arm PEG-vinyl sulfone (VS), and 10kDa 4-arm PEG-Ortho-Pyridyldisulfide (OPSS) dissolved in PM74 medium for 2 hours before being transferred into fresh PM74 medium for tracking of biomass accumulation. 4-arm PEG MAL has slight effects on the growth ($P < 0.05$ at time = 3 days) but 4-arm PEG-VS and 4-arm PEG-OPSS has significant effects ($P < 0.001$) the overall of growth of *Chlorella.*

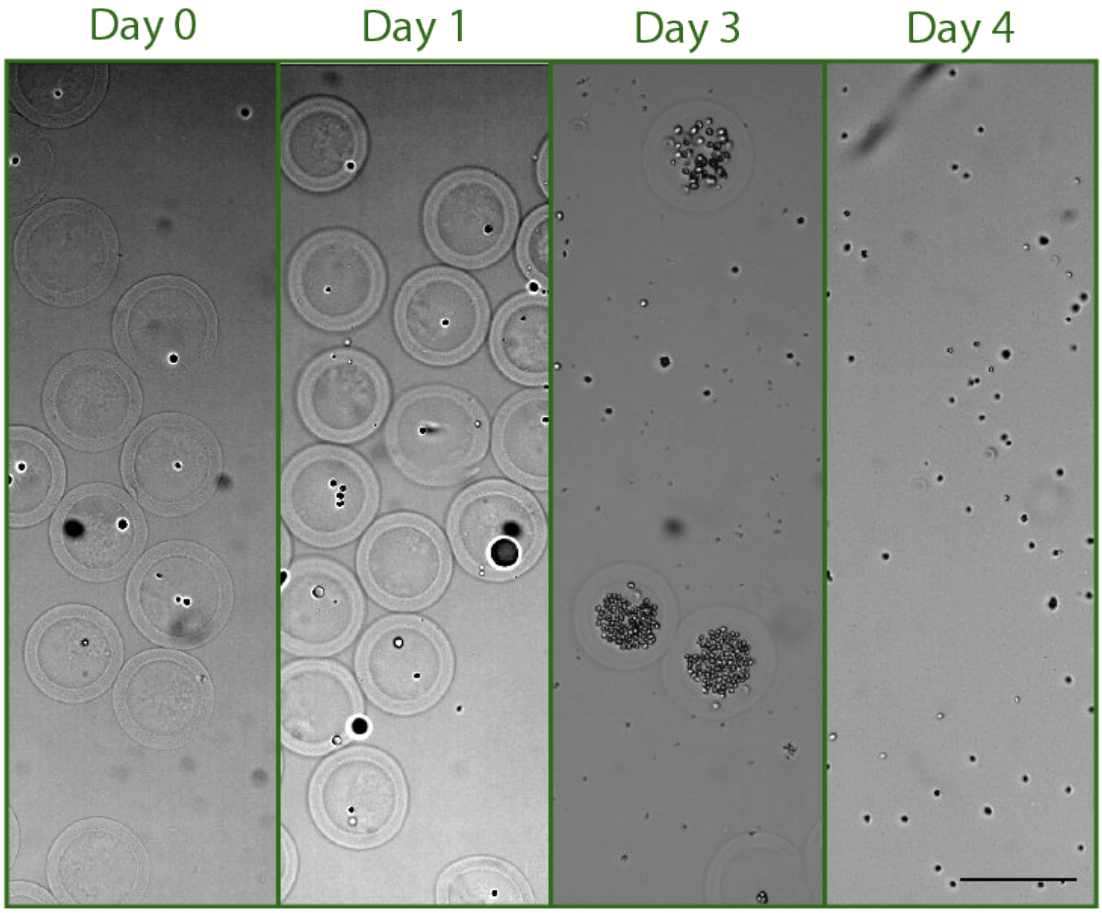

Figure S18. Growth of *Chlamydomonas reinhardtii* in MMP-degradable shells. *C. reinhardtii* are capable of growing in PicoShells crosslinked with MMP-degradable peptide crosslinker. However, cells pre-maturely induce the degradation of the PicoShells over time. This is likely due to natural MMPs secreted by *C. reinhardtii*. Scale bar = 100μm.

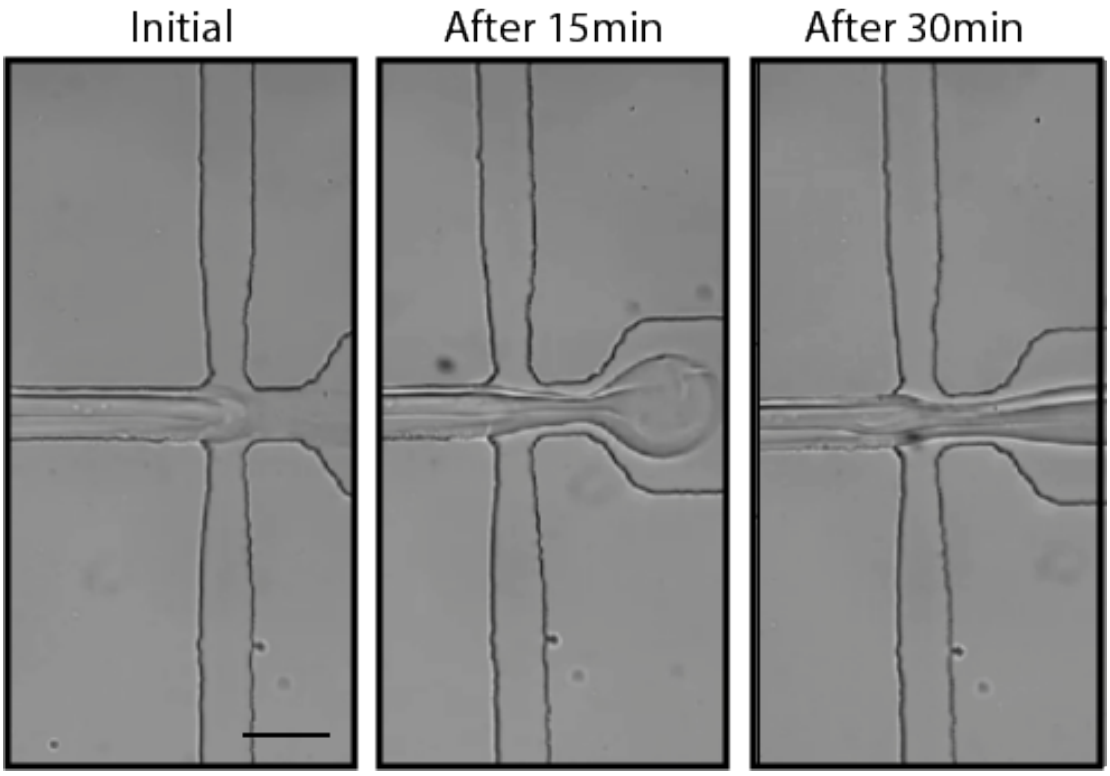

Figure S19. Disruption of PicoShell generation over time. Crosslinked material tends to form in the droplet generation junction over time, causing droplet formation to be disrupted. At a pH of 6.5, this usually starts to occur ~15 min after droplet generation is initiated when oversized droplets start to form. After ~30min, no droplets form. The time between initial mixing of reagents and jetting shortens as the pH of the solutions is increased. Scale bar = 100μm.

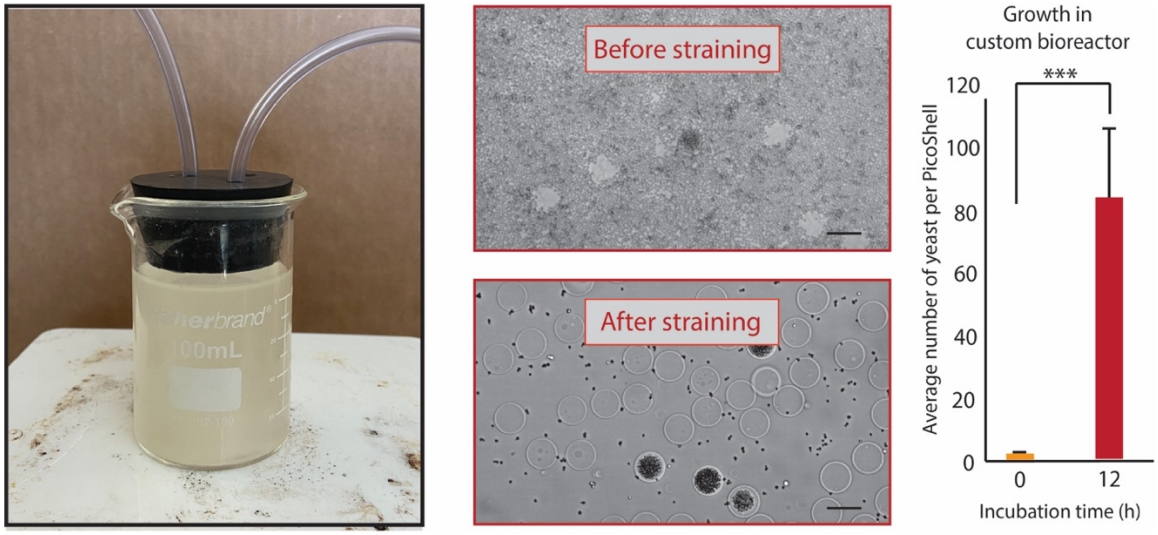

Figure S20. Incubation of PicoShells within a custom bioreactor. Individual *S. cerevisiae* were placed into PicoShells and placed into a custom bioreactor. The custom bioreactor was composed of a 100 mL beaker that had been sterilized and sealed with a rubber stopper. Two tubes ran completely through the rubber stopper into the bioreactor to allow gas exchange. The bioreactor also contained a stir bar rotating at 300 RPM and sat on a hot plate set to 30°C. The PicoShells were placed into the bioreactor with un-encapsulated *S. cerevisiae* for 12h. After the incubation period, the un-encapsulated cells were removed by passing the sample through a 20 µm cell strainer. PicoShells were recovered by inverting the strainer and flushing. 200 PicoShells were counted manually before and after incubation. There was a statistically significant difference ($P < 0.001$) in the number of cells per PicoShell before and after incubation. The average number of cells per PicoShell before incubation was 1.1 cells/PicoShell and after incubation was 84.5 cells/PicoShell. Error bars represent the standard deviation in the number of cells per PicoShell. Scale bars = 100 µm.

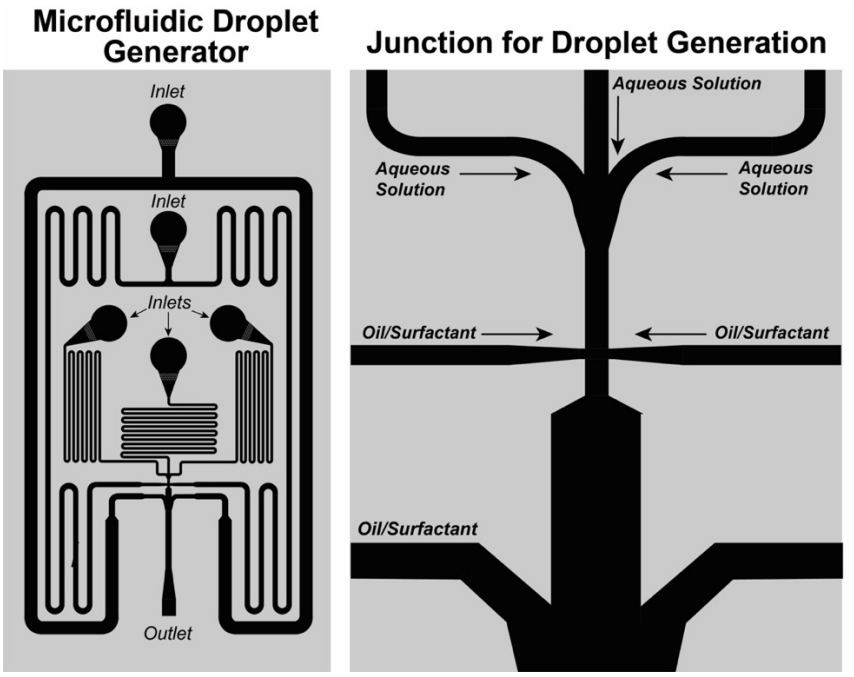

Figure S21. PicoShell and droplet generator design. The width of the channel at the junction for droplet generation is 60μm. The height of the channel at the junction is 70μm.

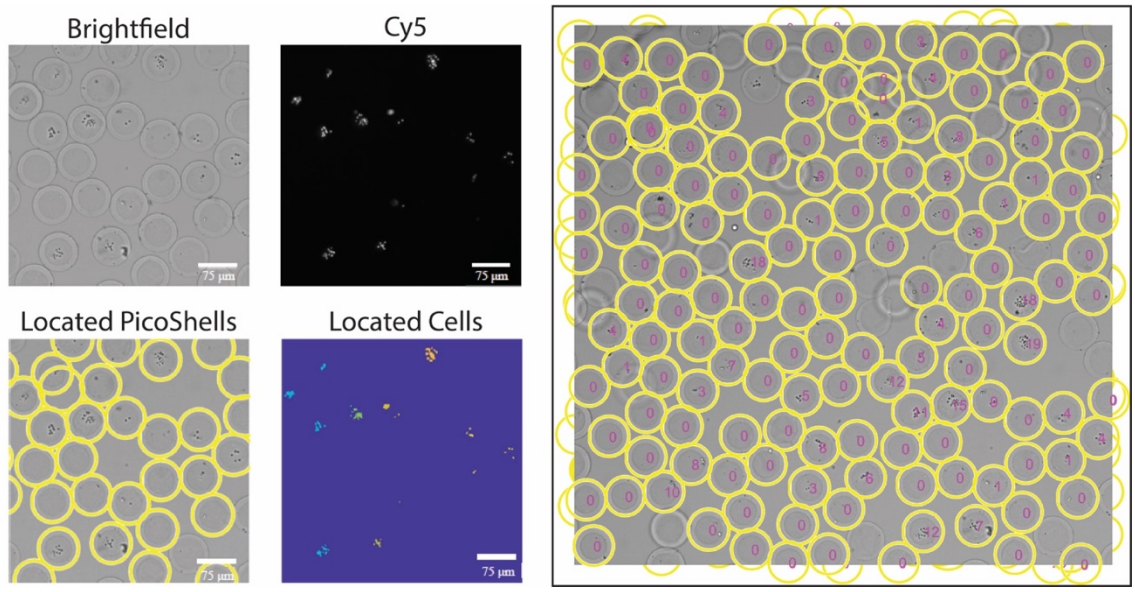

Figure S22. MATLAB code for cell counting of *Chlorella sp.* in PicoShells. PicoShells were located using the FindCircles function in the brightfield channel. A fluorescence overlay was used to find the *Chlorella sp.* using the chlorophyll fluorescence in the Cy5 channel. The number of cells was calculated by taking the area of each blob and dividing it by the 2D area of each cell within the compartment region. Some of the cells in PicoShells were counted visually to verify the accuracy of the code. After counting the *Chlorella* in 200 cell-containing PicoShells, we found that the difference between the visual count and the count from the code is not statistically significant ($P > 0.05$).

Movie S1 (Separate File). ATPS and PicoShell formation in droplet generator. PEG and dextran concentrations are fine-tuned such that a dextran-rich phase forms in the center of the droplet and a PEG-rich phase forms at the droplet's aqueous-oil interface. Crosslinking begins while the droplet travels downstream of the location of droplet formation.

Movie S2 (Separate File). Growth of *Chlorella* in PicoShells. Noticeable division of *Chlorella* in PicoShells is observed over a 24-hour period.

Movie S3 (Separate File). PicoShell rupture due to *S. cerevisiae* biomass accumulation. After ~80 hours of *S. cerevisiae* growth following initial encapsulation, the yeast cells can accumulate sufficient biomass such that the PicoShell diameter stretches from ~90μm to ~500μm before rupturing.

Movie S4 (Separate File). Mechanical breakdown of PicoShells. *Chlorella*-containing PicoShells were compressed between a glass slide and cover slip. The cover slip was pressed down onto the particles and twisted to cause PicoShells to break apart and cells to be released.

Movie S5 (Separate File). Chemical breakdown of disulfide-linked PicoShells. PicoShells containing disulfide linkages can be dissolved with the addition of DTT.

Movie S6 (Separate File). Trypsin breakdown of MMP-degradable-peptide-linked PicoShells. PicoShells crosslinked with peptides can be broken down with the addition of proteases such as trypsin.

Movie S7 (Separate File). Encapsulation of *Chlorella* into PicoShells. Cells are placed into the dextran phase prior to PicoShell fabrication. *Chlorella* can be visualized in the Cy5 fluorescence channel during encapsulation.

Dataset S1 (Separate File). Code for cell counting in PicoShells.